IEEE Photonics Journal
An IEEE Photonics Society Publication

Open Access

Polar Coded OFDM Signal Transmission at the W-Band in Millimeter-Wave System

Volume 11, Number 6, December 2019

Li Zhao
You-Wei Chen
Wen Zhou
Run-Kai Shiu
Shuyi Shen
Yanfei Lu
Jianjun Yu
Gee-Kung Chang

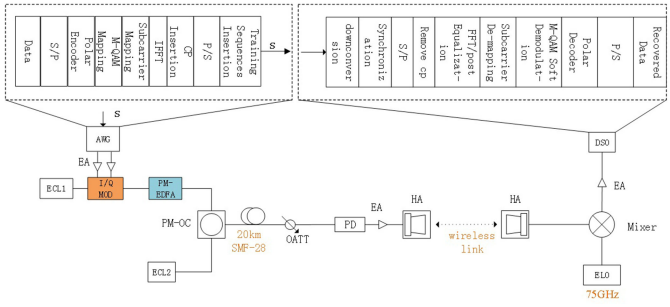

DOI: 10.1109/JPHOT.2019.2950407

Polar Coded OFDM Signal Transmission at the W-Band in Millimeter-Wave System

Li Zhao,[1,2] **You-Wei Chen**,[2] **Wen Zhou**,[1] **Run-Kai Shiu**,[2] **Shuyi Shen**,[2] **Yanfei Lu**,[2] **Jianjun Yu**,[1] **and Gee-Kung Chang**[2]

[1]Key Laboratory for Information Science of Electromagnetic Waves, Fudan University, Shanghai 200433, China
[2]School of Electrical and Computer Engineering, Georgia Institute of Technology, Atlanta, GA 30308 USA

DOI:10.1109/JPHOT.2019.2950407
This work is licensed under a Creative Commons Attribution 4.0 License. For more information, see https://creativecommons.org/licenses/by/4.0/

Manuscript received October 4, 2019; revised October 24, 2019; accepted October 26, 2019. Date of publication November 1, 2019; date of current version December 13, 2019. This work was partially supported by National Natural Science Foundation of China (NSFC) under Grants 61527801, 61675048, 61720106015, 61835002, and 61805043. Corresponding author: Li Zhao (e-mail: 1025350937@qq.com).

Abstract: We experimentally demonstrate the transmission of orthogonal frequency division multiplexing (OFDM) signals with polar codes FEC in a W-band MMW system. The BER performances of the M-QAM OFDM signal with FEC and without FEC are investigated, respectively. The experimental results show that the polar codes have a net gain of 7.9 dB compare with that of the LDPC code (7.4 dB). To the best of our knowledge, this is the first demonstration that the polar codes FEC are used in a W-band MMW system with OFDM modulation.

Index Terms: Orthogonal frequency division multiplexing (OFDM), polar code, M-ary quadrature amplitude modulation (M-QAM), millimeter-wave, W-band.

1. Introduction

The upcoming services, such as 4 K/8 K video and AR/VR services, are driving the capacity demand in the access network to grow at a very fast rate, which promotes the deployment of 5G communication. Millimeter-wave (MMW) communication plays an important role in 5G communications. Due to its short wavelength and wide available bandwidth, MMW can effectively solve many problems in current high-speed broadband wireless access systems, and it has exhibited a wide application prospect in short-distance communication [1]–[6]. Many applications based on the 5G MMW systems are proposed, e.g., 28 GHz [1], 60 GHz [2] and W-band MMW communication [3]–[6]. An FEC coding is mandatory to correct the error bits from an unreliable MMW channel to get an error-free threshold.

In 5G communication, there are two dominant FEC codes, which are polar codes and LDPC codes. The Coding and decoding design play a crucial role in ensuring that signals can be correctly restored. The performance of received signals via LDPC can further approach the Shannon capacity limit, and there is a 0.0045-dB gap between them [7]. On the other hand, polar codes proposed by E. Arikan are based on channel polarization [8], which can reach the Shannon capacity limit when polar coded signals are transmitted in a binary discrete memoryless channels at the an infinite length. In the optical communication system, the application of polar codes has been reported [9], and polar codes are used in OFDM system with intensity modulation and direct detection,

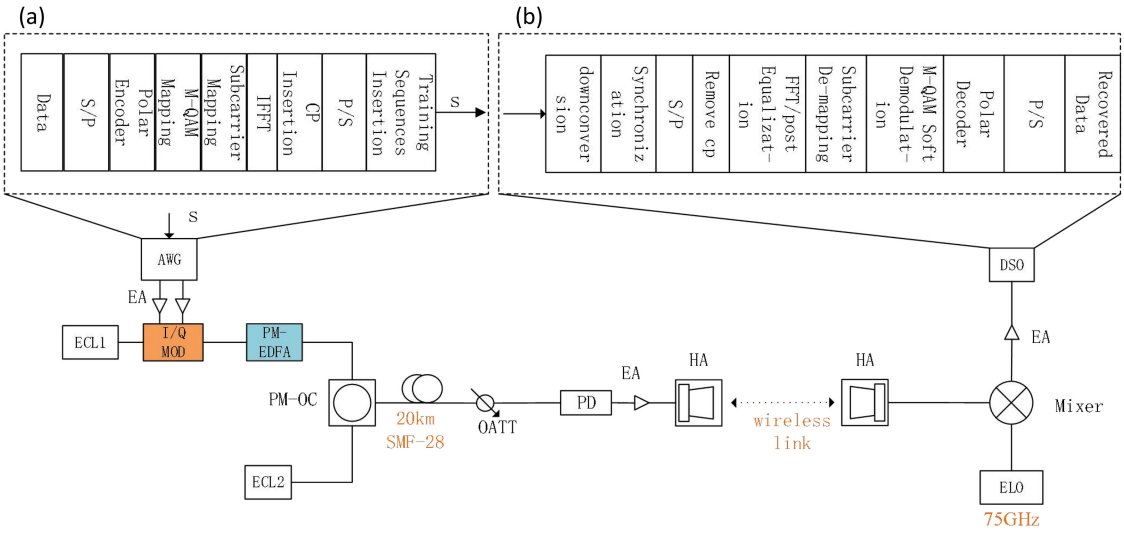

Fig. 1. Experimental setup for polar coded M-QAM OFDM heterodyne coherent detection. ELO: electrical local oscillator, HA: horn antenna, DSO: digital storage oscilloscope, PD: photodiode, OATT: optical attenuator, PM-OC: polarization-maintaining optical coupler, SMF-28: single-mode fiber-28, PM-EDFA: polarization-maintaining erbium-doped fiber amplifier, I/Q MOD: I/Q modulator, DAC: digital-to-analog converter, ECL: external cavity laser, and EA: electrical amplifier.

which shows 9.5-dB net coding gain (NCG) at the BER of 10^{-3} after 40-km single-mode fiber (SMF) transmission. However, it is more important to implement FEC codes in the 5G small cell densification environment since the wireless channel is much more unstable and suffers from multipath fading. Nevertheless, the investigation of the FEC codes in the W-band MMW fiber-wireless integration system has not been addressed. To further improve capacity and spectral efficiency, multi-carrier such as orthogonal frequency division multiplexing (OFDM) together with the high order quadrature amplitude modulation (QAM) format can be adopted.

In this paper, an experimental testbed of polar-coded M-QAM OFDM signals is demonstrated at W-band in MMW system. We experimentally demonstrated that the optimal length of the successive-cancellation list (SCL) [10] is 4 in this system. The experimental results show that with the aid of polar code and LDPC codes, the net gain of 7.9 dB and 7.4 dB can be achieved at the BER threshold of 1×10^{-3}, respectively. It is proved that polar codes are superior to LDPC codes when the code length is 1024 and the encoding rate is 0.5 at W-band in MMW system. To the best of our knowledge, this is the first time that the polar codes are used in the W-band MMW system.

2. Principle of Polar Code

Fig. 1 shows the experimental setup of polar coded OFDM signals transmission at W-band. The inset (a) in Fig. 1 depicts the generation of OFDM signals at the transmitter. Firstly, user data should be coded by polar codes. G_N is a generator matrix of size N [8].

$$G_N = B_N \times F^{\otimes n}, n = \log_2 N \text{ and } F^{\otimes n} = F \otimes F^{\otimes (n-1)} \tag{1}$$

$F = \begin{bmatrix} 1 & 0 \\ 1 & 1 \end{bmatrix}$ is operation for the joint channel. $\otimes n$ denotes the nth Kronecker power of the matrix. N denotes the code length of the polar codes. B_N is a bit-reversal permutation matrix.

$$B_N = R_N (I_2 \otimes B_{N/2}) \tag{2}$$

R_N is a permutation matrix, known as the reverse shuffle operation.

So we have an equation like this:

$$x_1^N = u_1^N G_N \tag{3}$$

u_1 is the binary original bit of the user, x_1 is polar coded bit sequence. Then $\sqrt{M}$ bits as a group are Gray mapping into the constellation of M-QAM. In order to produce OFDM signals, followed with subcarrier mapping, inverse fast Fourier transform (IFFT), addition of the cyclic prefixes (CP) with the length of 32, parallel to serial conversion. The length of subcarriers of OFDM signals is 1024, in which 4 low- frequency carriers are zeros for DC-bias, 980 carriers for data transmission, and the rest 40 carriers are null. There are 12 OFDM data symbols and 2 training sequences (TSs) in a frame of data. The 2 TSs are located in the front of a frame of data. The first one is used to synchronize data, and the second one is applied to channel estimation. The length of the polar code is 1024 and the code rate is 0.5. So the raw bit rate of 12Gbaud 16QAM is 48 Gb/s (12 $\times$ 4 Gb/s) and the net bit rate is 19.1 Gb/s (12 $\times$ 4 $\times$ (12/14) $\times$ (980/1056) $\times$ 0.5 Gb/s). The raw bit rate of 7Gbaud 64QAM is 42 Gb/s (7 $\times$ 6 Gb/s) and the net bit rate is 16.7 Gb/s (7 $\times$ 6 $\times$ (12/14) $\times$ (980/1056) $\times$ 0.5 Gb/s). The raw bit rate of 2Gbaud 256QAM is 16 Gb/s (2 $\times$ 8 Gb/s) and the net bit rate is 6.4 Gb/s (2 $\times$ 8 $\times$ (12/14) $\times$ (980/1056) $\times$ 0.5 Gb/s).

At the receiver, the block diagram of the OFDM signals recovery is shown in the inset (b) of Fig. 1. Firstly, the IF signals will be down-converted to baseband signals. Then, the baseband signals are recovered by implementing synchronization, serial-to-parallel conversion, CP removal, fast Fourier transform (FFT), channel equalization, subcarrier de-mapping, M-QAM soft demodulation, polar decoding, and parallel-to-serial conversion. The bit error rate is then calculated by comparing the bits of the transmitter and receiver.

In polar decoding, the method of SCL decoding is adopted to recover the original bit sequence. SCL decoder in [10] was improved from the original SC decoding [8]. Assume that $y = (y_0, y_1, y_2 \ldots y_{n-1})$ is the corresponding channel output and $\hat{u_0}$, $\hat{u_1}$, $\hat{u_2} \ldots \hat{u_{n-1}}$ is estimated from u_0, u_1, $u_2 \ldots u_{n-1}$. For $c \in \{0, 1\}$, we have the probability of $\Pr(y|\hat{u}_0^{i-1}, u_i = c)$ when y was received, on the condition that $u_i = c$ and $u_0^{i-1} = \hat{u}_0^{i-1}$. The estimated value $\hat{u_i}$ can be chosen according to

$$\hat{u_i} = \begin{cases} 0 & \text{if } \frac{\Pr\left(y|\hat{u}_0^{i-1}, u_i=0\right)}{\Pr\left(y|\hat{u}_0^{i-1}, u_i=1\right)} \geq 1, \\ 1 & \text{otherwise.} \end{cases} \tag{4}$$

The process of SCL decoder is similar to the SC decoder, except that the decoder retains both possible estimates, $\hat{u_i} = 0$ and $\hat{u_i} = 1$, in the subsequent decoding paths. The basic idea of SCL decoding algorithm is to find the most suitable path and obtain the decoding sequence in a full binary tree formed by polar codes according to the principle of the maximum posterior probability. The height of the code tree formed by polar codes with code length is N, the depth of root node is 1, and the depth of leaf node is N. Each node in the tree represents a bit, and there are 2^{i-1} nodes in layer i, representing the value of the bit u_i given all possible values of $\hat{u}_0^{i-1}$. A node with a depth of d and a node with a depth of $d + 1$ are connected by two edges, representing two paths of $u_d = 0$ and $u_d = 1$ respectively. At each level of the tree, the path is sorted, selected and cleaned according to the size of the path measurement value of each path.

3. Experimental Setup

Fig. 1 demonstrates the experimental setup of W-band system with heterodyne coherent detection. In the transmitter side, M-QAM baseband signals are produced from 12 Gsa/s arbitrary waveform generator (AWG), it will be used to drive in-phase/quadrature (I/Q) modulator after they are amplified by two parallel amplifiers. The I/Q modulator has 32 GHz 3 dB bandwidth which is used for M-QAM modulation with 6 dB insertion loss. ECL1 and ECL2 have 13 dBm output power and $<$100 kHz linewidth. ECL1 and ECL2 are used as a signal source and an optical local oscillator (LO), respectively. A continuous lightwave produced from ECL1 is loaded into I/Q modulator to modulate the electrical baseband OFDM signal. We will adopt a polarization-maintaining Erbium-doped

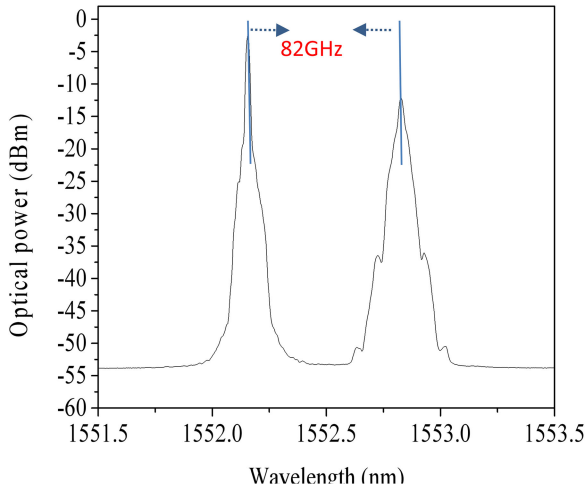

Fig. 2. Measured optical spectrum.

fiber amplifier (PM-EDFA) in order to amplify the optical signal output from I/Q modulator. Before optical signal transmitted through a 20 km single-mode fiber, two laser beams will be coupled by a polarization-maintaining optical coupler (OC). 82-GHz M-QAM signal at W-band can be achieved after heterodyne beat via a PD. The PD has ∼100 GHz optical bandwidth, and the inputpower of which can be adjusted by an optical attenuator. Before the signals are transmitted into horn antenna (HA) with 25 dBi gain, it will be amplified by a W-band electrical amplifier (EA) with 10 dBm saturation output power and 25 dB gain. Then the signals will be delivered into free space through HA. The optical spectrum (0.01-nm resolution) of the 16QAM OFDM signals after the PM-OC is depicted in Fig. 2.

4. Experimental Results

The received power P_R after wireless transmission based on the following Friis transmission equation [6]:

$$P_R(dB) = G_T + G_R + P_T - 20\log\left(\frac{4\pi d}{\lambda}\right) - L_A \times d - L_F \tag{5}$$

Where transmitter/receiver antenna gain is GT/GR , PT is a transmitter power, and d is wireless transmission distance. LA is the atmospheric loss factor at W-band, which is 0.4 dB/km on a sunny day. The loss of antenna feedback is LF and the transmission wavelength is λ. The path loss is about 93 dB for at 13 m wireless mm-wave delivery. In our experiment, PT is 9 dBm, GT and GR are both 25 dBi, and LF is 3 dB, so the predicted received power is -37.3 dBm for 13 m wireless mm-wave delivery at an 82 GHz center frequency. The measured received power is -39 dBm, which is close to the predicted received power of -37.3 dBm.

Fig. 3(a) shows the curves of BER versus received optical power (ROP) at different length of SCL when 12-Gbaud 16QAM OFDM signals are transmitted in 1-m wireless and 20-km SMF. As we can see from Fig. 3(a), with the increase of ROP, BER decreases gradually. And we can see that with the increase of the length of SCL, the BER performance will become better. However, the increase of the length of SCL will put more complexity to the algorithm [10]. And we can see that the length of 4, 8, 12 has the same BER performance, so the length of 4 is the best choice. The following experimental results are based on length 4.

The curves of ROP versus BER are depicted in Fig. 3(b) when 12-Gbaud 16QAM OFDM signals are transmitted in 1-m wireless and 20-km SMF. In order to better verify the performance of polar codes, we first compared the computational complexity of polar and LDCP codes, and then we

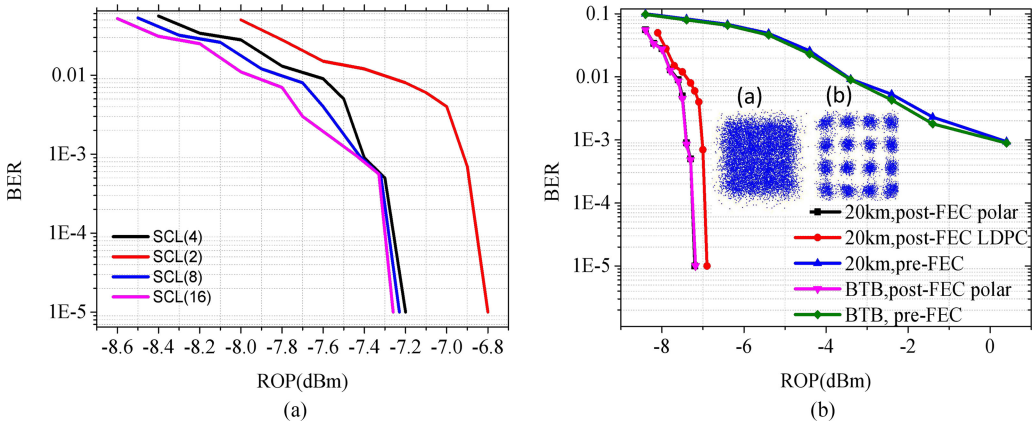

Fig. 3. (a) BER vs ROP at different length of SCL. (b) BER versus input power of 16QAM OFDM signal with 1 m wireless link. Constellations at ROP of (a) −7.2 dBm and (b) 0.4 dBm.

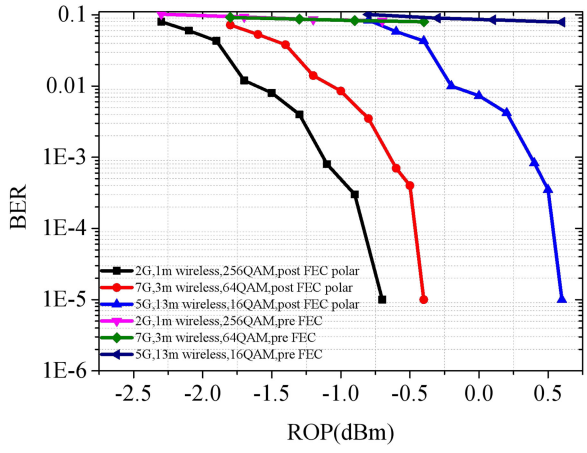

Fig. 4. BER versus ROP of 16QAM, 64QAM, 256QAM OFDM signal with 13 m, 3 m, 1 m wireless link.

compare the improvement of system performance when the two algorithms are used in W-band MMW system. The LDPC encoding with a specific parity matrix, decoding with iterations of the belief propagation algorithm, and the length of iterations (r) is 50 in our experiment. LDPC codes have the computational complexity of encoding $O(N^2)$ and decoding $O(r * N)$ respectively, and polar codes have the computational complexity of encoding $O(N * \log N)$ and decoding $O(L * N * \log N)$ respectively. More detailed discussion is presented in [8], [10], [11]. The BER performance is compared at pre-FEC and post-FEC in Fig. 3(b), and the performance of LDPC and polar code is compared at the same code length and code rate. As we can see from Fig. 3(b), with the increase of ROP, BER performance becomes better. For the curves without FEC code, with the increase of ROP, BER slowly getting better. Moreover, due to the limitation of experimental equipment, ROP will reach the threshold of the saturation power of PD when the ROP increases to a certain value. Therefore, when ROP is increased to 0.4 dBm, BER performance could not be improved continuously. However, as for the curves with FEC, we can see from Fig. 3(b) that the BER can be quickly improved, and achieve a low value. It is also worth noting that the BER performance improve ment by the polar FEC is better than LDPC FEC. Fig. 3(b) shows that the net gain of 7.9 dB and 7.4 dB can be achieved at the BER threshold of 1×10^{-3} with the help of polar codes and LDPC codes, respectively. Inset (a) and (b) in Fig. 3(b), which are the constellation diagram when ROP is −7.2 and 0.4 dBm, respectively, which has BER of 7.9×10^{-2} and 9.4×10^{-4}, respectively. When ROP is −7.2 dBm, with the help of polar code, BER can reach a small threshold value of

1×10^{-5}. From the experimental results, we can conclude that polar codes are suitable for W-band MMW systems. In order to further show the advantages of polar in the W-band MMW system, and to maximize the transmission capacity as well as wireless transmission distance of the system, we explored combinations of different wireless transmission distance and different QAM modulation formats in order to meet the requirements of different 5G application scenarios in the future.

Fig. 4 shows the curves of BER versus ROP with different QAM modulation. As we can see from Fig. 4, with the increase of ROP, the BER performances of all curves become better. However, with the increase of power, the power will reach the saturation threshold of the PD. When the power exceeds the saturation threshold of the PD, the BER performance will not be improved. However, with the help of polar code, the BER quickly reaches a very low value of 1×10^{-5}. For 1-m wireless delivery, we can get a raw bit rate of 16 Gb/s (2×8) for 256QAM signal transmission. For 3-m wireless delivery, we can realize a raw bit rate of 42 Gb/s(7×6) for 64QAM signal delivery . For 13-m wireless delivery, we can obtain a raw bit rate of 20 Gb/s(5×4) for 16QAM signal delivery.

5. Conclusion

For the first time, the polar codes FEC has been demonstrated in a W-band MMW system. The optimal length of the successive-cancellation list (SCL) is 4 in the MMW system. The BER performance with FEC or without FEC M-QAM OFDM is investigated. The polar codes have a net gain of 7.9 dB compare with LDPC code of 7.4 dB at the BER threshold of 1×10^{-3}.

References

[1] R. Shiu *et al.*, "Tunable microwave photonic filter for millimeter-wave mobile fronthaul systems," in *Proc. IEEE Photon. Conf.*, 2018, pp. 1–2.
[2] Y. Chen *et al.*, "A reliable OFDM based MMW mobile fronthaul with DSP-aided sub-bandspreading and time-confined windowing," *J. Lightw. Technol.*, vol. 37, no. 13, pp. 3236–3243, Jul. 2019.
[3] X. Li, J. Yu and G.-K. Chang, "Photonics-assisted technologies for extreme broadband 5G wirelesscommunications," *J. Lightw. Technol.*, vol. 37, no. 12, pp. 2851–2865, Jun. 2019.
[4] L. Zhao, Y. Zhang, and W. Zhou, "Probabilistically shaped 64QAM OFDM signal transmission in a heterodyne coherent detection system," *Opt. Commun.*, vol. 434, pp. 175–179, 2019.
[5] X. Pang *et al.*, "100 Gbit/s hybrid optical fiber-wireless link in theW-band (75–110 GHz)," *Opt. Exp.*, vol. 19, no. 25, pp. 24944–24949, 2011.
[6] X. Li, J. Xiao, and J. Yu, "Long-distance wireless mm-wave signal delivery at w-band," *J. Lightw. Technol.*, vol. 34, no. 2, pp. 661–668, Jan. 2016.
[7] S. Y. Chung, G. D. Forney Jr., T. J. Richardson, and R. Urbanke, "On the design of low-density parity-check codes within 0.0045 dB from the Shannon limit," *IEEE Commun. Lett.*, vol. 5, no. 2, pp. 58–60, Feb. 2001.
[8] E. Arikan, "A method for constructing capacity-achieving codes for symmetric binary-input memoryless channels," *IEEE Trans. Inf. Theory*, vol. 55, no. 7, pp. 3051–3073, Jul. 2009.
[9] J. Fang *et al.*, "Performance investigation of polar coded IM/DD optical OFDM for short reach interconnection," in *Proc. Opto-Electron. Commun. Conf. Photon. Global Conf.*, 2017, pp. 1–3.
[10] I. Tal and A. Vardy, "List decoding of polar codes," *IEEE Trans. Inf. Theory*, vol. 61, no. 5, pp. 2213–2226, May 2015.
[11] B. Liu, L. Zhang, X. Xin, and J. Yu, "Robust generalized filter bank multicarrier based optical access system with electrical polar coding," *IEEE Photon. J.*, vol. 8, no. 5, Oct. 2016, Art. no. 7906507.